COBEM 2023 27TH INTERNATIONAL CONGRESS OF MECHANICAL ENGINEERING

ABCM Brazilian Society of Mechanical Sciences and Engineering
27th ABCM International Congress of Mechanical Engineering
December 04-08, 2023, Florianópolis-SC, Brazil

COB-2023-2421
FABRICATION OF MULTI-SCALE PERIODIC LINE-LIKE STRUCTURES ON DIFFERENT IMPLANT MATERIALS USING A TWO-BEAM INTERFERENCE SETUP EQUIPPED WITH A PICO-SECOND LASER SOURCE

Bruno Henriques
Ceramic and Composite Materials Research Group (CERMAT), Federal University of Santa Catarina (UFSC), 88040-900, Florianópolis, SC, Brazil
Center for Micro-Electro Mechanical Systems (CMEMS-UMinho), University of Minho, Campus de Azurém, 4800-058 Guimarães, Portugal

Bodgan Voisiat
Institute for Manufacturing Technology, Technische Universität Dresden, George-Baehr-Str.3c, 01069 Dresden, Germany
bogdan.voisiat@tu-dresden.de

Douglas Fabris
Ceramic and Composite Materials Research Group (CERMAT), Federal University of Santa Catarina (UFSC), 88040-900, Florianopolis, SC, Brazil
douglas.df1@gmail.com

Andrés Fabian Lasagni
Institute for Manufacturing Technology, Technische Universität Dresden, George-Baehr-Str.3c, 01069 Dresden, Germany
andres_fabian.lasagni@tu-dresden.de

Abstract. *Surface topography modifications are well-established strategies to improve the biological response of biomaterials and their performance and reliability when used as implants. Studies have shown that surface roughening creates a physical anchorage between the implant and bone and improves its primary and long-term stabilization. Cell proliferation, protein synthesis and cell growth direction can be controlled with well-defined micro- and nanotexture. Conventional techniques to introduce micro- and nanofeatures include acid etching, micromachining, grinding and grit-blasting. Although widely used, these techniques present drawbacks that limit their use in advanced engineering applications. Direct Laser Writing (DLW) has emerged as a powerful alternative. In this technique, the feature resolution is limited by the laser beam diameter (usually 5-10 μm). On the other hand, the Direct Laser Interference Patterning (DLIP) technique takes advantage of the physical principle of interference to produce features with spatial resolution similar to the laser wavelength. In this method, the laser is split into two or more beams, which are superposed on the material surface, creating an interference pattern. At the maxima regions, the high energy density causes ablation, while the material is not affected at the minima regions, resulting in periodic structures on the surface.*
In this work, DLIP method is used for the fabrication of well-defined and flawless multi-scale surface structures in biomedical materials, including zirconia, polyether-ether-ketone (PEEK), AZ91D magnesium alloy, and Cobalt-Chromium-Molybdenum (CoCrMo). A two-beam interference configuration is used, together with an ultrashort pulsed laser, producing high-quality line-like patterns with a period of a few micrometers. Confocal and Scanning Electron Microscopes are utilized to analyze the topography of the manufactured structures, observing significant differences based on the applied process parameters.

Keywords: *Microfabrication, surface structuring, zirconia, Direct Laser Interference Patterning*

1. INTRODUCTION

The arrangement of small structures on a material's surface has a significant impact on how it behaves in its surroundings. This arrangement can be adjusted to enhance how the material performs its intended task. The surface structure affects properties like how easily liquids spread on it, how well it sticks to other surfaces, its resistance to sliding, its appearance, and how it resists wear and damage. These surface features also maintain the material's desired properties throughout its bulk (Brown and Arnold, 2010) For example, specific surface roughness can improve the bond between two materials by creating a mechanical lock. Adjusting the surface can also make it repel or attract water (Watanabe et al., 2012). In medical materials, having different-sized features oriented in specific ways can make implants interact better with tissue, mimicking a natural cell environment (Dumas et al., 2012).

Traditional methods to create these tiny structures include using chemicals to etch the surface, cutting it at a small scale, grinding it, or shooting small particles at it. However, these methods have limitations for advanced engineering uses. They can only create random structures with little control over their size and shape (Le Guéhennec et al., 2007). Making patterns smaller than 100 μm is hard, and so is working with hard and brittle materials. In advanced engineering, it's crucial to control the size and direction of these features. For instance, having random roughness on an implant can lead to more bacteria, but controlled, very small structures can reduce bacterial attachment (Bohinc et al., 2014; Cunha et al., 2016). The direction of these tiny structures can also guide how cells grow (Lukaszewska-Kuska et al., 2018). Moreover, they affect how the material wears down and how much friction it generates when it rubs against another material. Tiny grooves on the surface can trap lubricants and reduce friction. But if the grooves are too large, the lubricant flows away. So, the grooves have to be just right to keep the lubricant in place (Stark et al., 2019). In this context, a flexible method to create high-detail structures is using lasers. A strong laser can precisely remove a small amount of material from the surface. Lasers are fast and accurate and usually don't damage the surface much. Very short laser pulses (picoseconds and femtoseconds) are especially good at making almost flawless textures without causing cracks or melting because they remove a very thin layer of material (Bauer et al., 2015).

One method called Direct Laser Writing (DLW) is useful for creating small patterns on the surface. However, its accuracy is limited by the size of the laser beam (which can't easily go smaller than 5-10 μm) (El-Khoury et al., 2020). Another method called Direct Laser Interference Patterning (DLIP) uses the interference of multiple laser beams to create patterns as small as the laser's wavelength. The beams overlap on the material's surface, creating regions where the energy is high enough to remove material (resulting in patterns) and regions where the material isn't affected (resulting in gaps in the pattern). The size of the pattern depends on things like the angle between beams, the laser's strength, and how the laser pulses interact with the material (Mücklich et al., 2006).

DLIP has been studied on many materials, especially metals. But there isn't much research on using DLIP on CoCrMo and AZ91D magnesium alloys. AZ91D is a common magnesium alloy with added aluminum and zinc for strength and corrosion resistance. CoCrMo alloy has good properties too, like strength, wear resistance, and compatibility with the body. DLIP has been suggested to help recovery on heart stents made from CoCr alloy. However, there isn't information on using DLIP on AZ91D. Results on DLIP on other biomaterials such as zirconia or PEEK are also very scarce. Therefore, this study aimed to use DLIP to add texture to CoCrMo, AZ91D, PEEK and Zirconia (3Y-TZP) surfaces while exploring how different laser parameters affect the surface's morphology.

2. MATERIALS AND METHODS

Experiments involving laser-based surface structuring were conducted on two types of materials: polished CoCrMo alloy and AZ91D alloy. The CoCrMo alloy had the following composition: 63% cobalt (Co), 24% chromium (Cr), 3% molybdenum (Mo), 8% tungsten (W), 1% silicon (Si), and 1% niobium (Nb). The alloy was in the form of disks with a diameter of 10 mm and a thickness of 4 mm. The AZ91D alloy composition consisted of 90% magnesium (Mg), 9% aluminum (Al), and 1% zinc (Zn). Plates of this alloy were 3 mm thick. Before the laser texturing process, the samples underwent ultrasonic cleaning in isopropyl alcohol for 10 minutes, followed by rinsing in distilled water to eliminate contaminants.

The laser structuring was carried out using the Direct Laser Interference Patterning (DLIP) technology (Figure 1). The DLIP system utilized was equipped with a 10 picosecond solid-state Nd:YVO4 laser (PX200, EdgeWave, Würselen, Germany) with a maximum output power of 10 watts. The laser operated at a wavelength of 1064 nanometers, with a fixed repetition rate of 10 kHz and a Gaussian beam profile. The setup employed a diffractive optical element (DOE) to split the main laser beam into two sub-beams with equal angles to the optical axis. These sub-beams were parallelized using a prism and then focused and overlapped onto the sample surface using a 60 mm focal length aspheric lens. This arrangement generated an interference pattern in the form of a line-like profile on the sample's surface.

The interference pattern was created by overlapping the two laser sub-beams at an angle of 24 degrees on the sample's surface, resulting in a spatial period (distance between pattern repetitions) of 5.0 micrometers. This spatial period was determined by the relationship between the laser wavelength and the angle between the interfering beams. The interference pattern was transferred onto the material surface through selective laser ablation at the regions of maximum intensity in the interference profile.

To create larger textured lines or areas, the samples were moved in the x and y directions using high-precision positioning axes. For instance, in this study, long lines were textured by moving the sample in the y-direction with each laser pulse. The overlap between successive laser pulses (pulse-to-pulse overlap) was controlled by adjusting the distance between the pulses. Higher overlap percentages corresponded to more pulses hitting the same area. Different combinations of laser fluence (energy per unit area) and pulse-to-pulse overlap were tested for both CoCrMo and AZ91D materials to observe the resulting changes in surface structure. The laser experiments were conducted in an ambient environment, and no further treatments were applied after the laser structuring process.

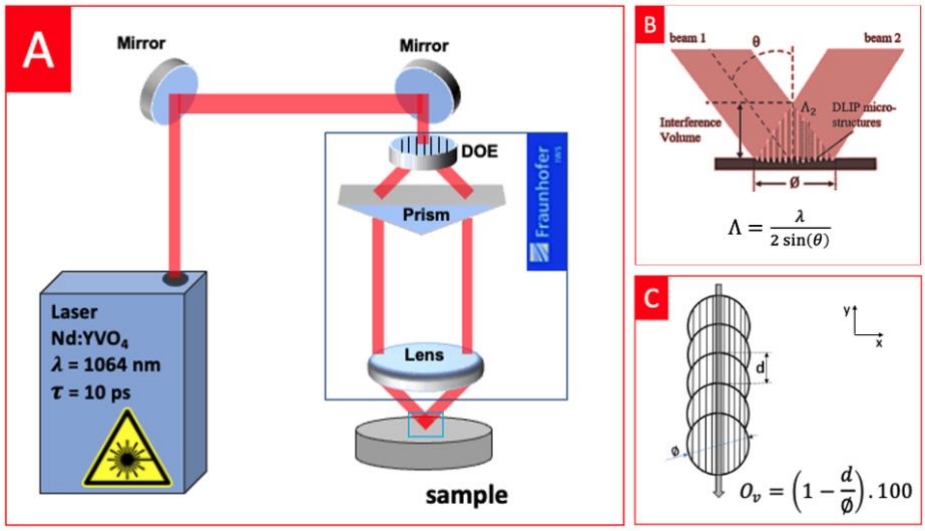

Figure 1. (A) DLIP system optical setup; (B) interference pattern created by the overlap of the sub-beams: ablation occurred mainly at the maxima regions, creating line-like patterns with pe-riod Λ; (C) line-like texturing strategy used on this work. Adapted from (Henriques et al., 2023a), Copyright (2023), with permission from Elsevier.

Confocal Microscopy (S-Neox, Sensofar, Barcelona, Spain) employing 150× objective was used to analyse the surface topography, resulting in a vertical resolution of 2 nm and a lateral resolution of 140 nm. The acquired topographical data were processed using the software MountainsMap 7.4 (Digital Surf, Besançon, France), which calculated the average depth of the fabricated structures. The surface morphology of the specimens was also analysed using a Scanning Electron Microscope (JSM-6010 LV, JEOL, Tokyo, Japan) op-erating at an accelerating voltage of 5.0 kV with magnifications between 5000× and 20 000× and using Secondary Electrons. Furthermore, the chemical composition of the samples (before and after laser texturing) was analysed using Energy Dispersive Spectroscopy (EDS) accessory at an accelerating voltage of 15 kV. These analyses were performed approximately at the centre of the textured region.

3. RESULTS AND DISCUSSION

Various line-like structures with a periodicity (distance between pattern repetitions) of Λ = 5.0 µm were successfully generated using different laser settings. The experiments were designed to investigate how the deposited energy affects both the average depth of the created structures and the overall surface morphology. To achieve this, the impact of two laser parameters, namely laser fluence (energy density delivered by a single laser pulse) and pulse overlap (number of pulses striking the same spot), was studied.

3.1. CoCrMo Alloy

The CoCrMo alloy was used for the experiments, and the results of the average structure depths achieved under different fluence and pulse overlap conditions are depicted in Figure 2. A general trend is evident from the dashed lines on the graph: increasing either the pulse fluence or the overlap leads to a rise in the depth of the features. This implies that, within the tested conditions, employing higher energy over the same area results in the creation of deeper structures. For instance, at a fluence of 13.3 J/cm², the average depth increases from 0.30 µm with an 85% overlap to 0.85 µm with a 98% overlap. Similarly, when the overlap is fixed at 98%, varying the fluence from 3.8 J/cm² to 13.3 J/cm² leads to an increase in structure depth from 0.40 µm to 0.85 µm. This trend agrees well with findings from other studies involving different materials (Aguilar-Morales et al., 2018; Henriques et al., 2023a; Mulko et al., 2022).

The depths achieved in this research are consistent with those presented in the study by Schieber et al., although their work indicated that the conditions required to achieve such depths caused the entire surface to remelt (Schieber et al., 2017). While the tested conditions on the CoCrMo alloy did not exhibit this behavior, it's worth noting that excessive laser energy can have adverse effects. Specifically, excessively high energy levels can cause the depths of the grooves to decrease or even result in their destruction. Moreover, excessive energy can lead to the heating and melting of the surface layer at points of destructive interference. This can cause molten material to flow into the grooves and accumulate within the cavities.

Importantly, it should be noted that the reported depths were measured at the center of the laser beam. Given the Gaussian nature of the beam, the depth tended to decrease towards the outer edges of the beam.

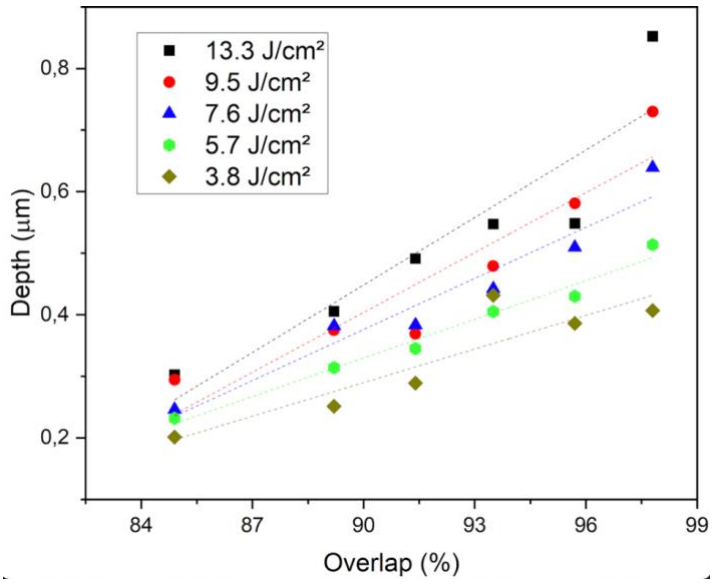

Figure 2. Average depth and standard deviation of line-like structures obtained by DLIP on CoCrMo surfaces for different combinations of pulse overlaps and laser fluence. Reprinted from (Henriques et al., 2023b), Copyright (2023), with permission from MDPI.

The SEM images presented in Figure 2 showcase the surfaces of CoCrMo samples that underwent DLIP modification under varying laser processing conditions. These images shed light on the effects of different energy levels on the resulting structures. When energy levels are kept low (associated with low fluence and/or overlap), it is not only evident that the structures possess shallow depths, as depicted in Figure 2, but it is also noticeable that the grooves, where the interference pattern reaches its peak, are notably narrow compared to the ridges. As the fluence and/or overlap values are elevated, the width of the grooves expands in tandem with their depth, culminating in more clearly defined structures.

Furthermore, it is observable that the process of ablation extended throughout the entire region underneath the laser beam, even encompassing the minima positions (ridges) of the interference pattern. This phenomenon indicates that the heat introduced in the maxima regions was conducted excessively, surpassing the material's threshold for ablation. To exclusively achieve ablation at the maxima positions, lower energy levels would need to be utilized. However, this would come at the expense of reducing both the depth and the precision of the features.

The SEM images also expose the presence of smaller features resembling ripples on the sample's surface, particularly noticeable under high-overlap conditions (above 94%). Upon closer inspection at higher magnification (as depicted in Figure 2) on the sample subjected to a laser fluence of 7.6 J/cm² and 98% overlap, these secondary sub-micrometric structures become discernible across the entire textured surface. These structures, aligned parallel to the DLIP structures, fall under the classification of laser-induced periodic surface structures (LIPSS). Notably, they exhibit a spatial frequency of approximately 1000 nm, which closely mirrors the laser wavelength of 1064 nm.

Despite their diminutive size, these structures wield the capacity to induce alterations in optical, mechanical, and chemical properties of the surface. Research has indicated that LIPSS can diminish bacterial adherence to titanium implant surfaces while simultaneously enhancing cell differentiation—a factor that can enhance the overall performance of implants. Prior studies by Batal et al. exhibited that laser-textured CoCrMo implants demonstrated improved initial cell adhesion due to heightened roughness, but the presence of submicrometric features (LIPSS) further bolstered both cell adhesion and proliferation. In our study, the coexistence of multiscale surface structures could potentially amplify the cellular response to implant surfaces by leveraging a possible synergy between the grooves and the LIPSS. However, for a concrete understanding of this hypothesis and the biological reaction to multiscale texturing, further biological investigations are warranted.

Surface texturing can also exert a substantial influence on a material's tribological properties. Research has shown that textured grooves possess the capacity to harbor lubricants and capture wear debris, effectively reducing the coefficient of friction and wear rate. Furthermore, smaller feature sizes, characterized by periods smaller than 10 µm—such as those produced through DLIP—appear to exert a more favorable effect on diminishing friction in comparison to traditional Direct Laser Writing (DLW) techniques that result in larger periods exceeding 30 µm.

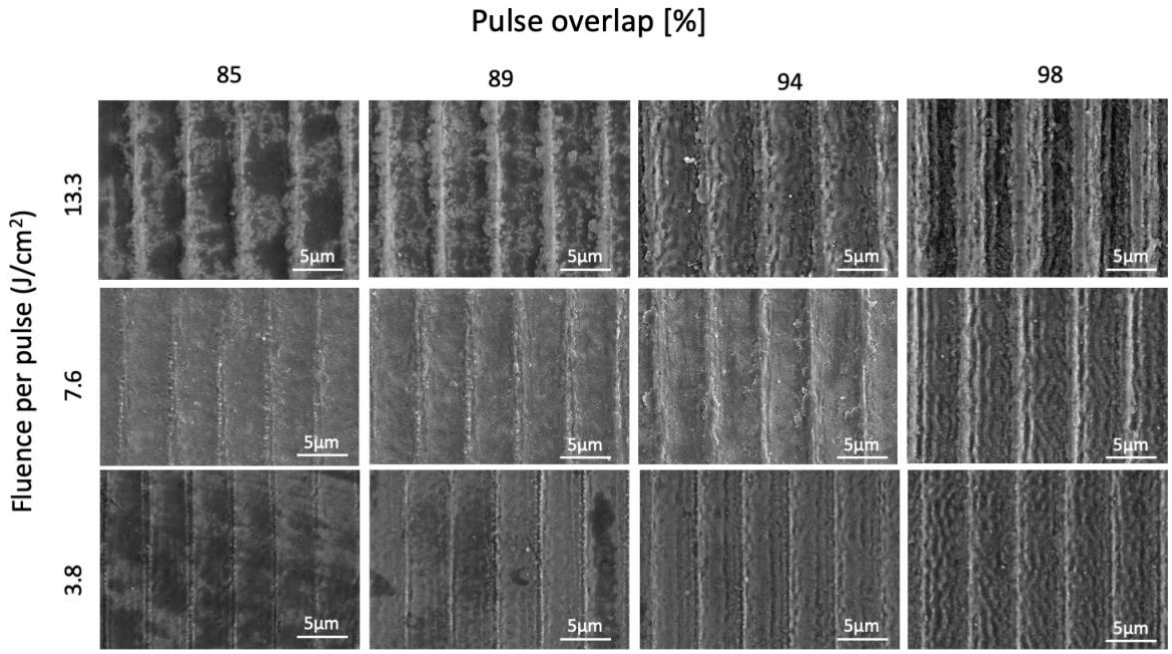

Figure 2. SEM images from the textured surface of the CoCrMo samples for different conditions tested. Reprinted from (Henriques et al., 2023b), Copyright (2023), with permission from MDPI.

3.2. AZ91D Alloy

The texturing process was effectively applied to the AZ91D magnesium alloy using the DLIP technique. As depicted in Figure 3, the figure illustrates the depth of various DLIP structures achieved through different combinations of laser fluences and pulse-to-pulse overlaps. A clear pattern emerges: the depth of structures escalates with increasing pulse overlaps, irrespective of the level of laser fluence employed. For instance, at a fluence of 0.9 J/cm², the depths of structures ascend from 0.9 µm to a peak of 2.5 µm (the maximum recorded depth) when the overlap transitions from 85% to 98%.

Furthermore, it is evident that at lower overlaps, reduced fluences result in shallower depths, while heightened fluences lead to deeper depths—precisely as expected and noted for the CoCrMo alloy. Nonetheless, a shift in this trend becomes apparent for higher overlaps, specifically above 96%. In these scenarios, lower fluences yield greater depth values, such as 0.9 J/cm² and 6.6 J/cm². This change in trend becomes more apparent through the linear fitting lines (represented as dashed lines on the graph), which exhibit a steeper slope for lower fluence values.

This observation hints at the occurrence of melting on the ridges at high energy levels (corresponding to high fluence and/or high overlap). This molten material flows into the surrounding region and accumulates within the grooves, ultimately leading to a reduction in the overall average depth. This phenomenon means that, unlike the CoCrMo alloy, further increases in energy might not necessarily result in deeper features. Nevertheless, it's noteworthy that the grooves created on the magnesium alloy were consistently deeper than those generated on the CoCrMo alloy, irrespective of the specific laser conditions utilized.

In Figure 4, SEM images showing the details of the DLIP-structured surfaces are presented. Under conditions of low overlap (85%) and low fluence (0.9 J/cm²), the initial stages of structure development are evident, although they lack well-defined features. The irregular shape of the lines, particularly noticeable at higher fluence levels, indicates the occurrence of melting on the ridges, compromising the overall clarity of the texture. However, at overlaps exceeding 94%, line-like periodic structures boasting a periodicity of $\Lambda = 5$ µm emerge with distinct definition and uniformity. The morphology of samples textured using elevated fluence and overlap values further aligns with the earlier discussion regarding the accumulation of melting within the grooves.

Under conditions of high fluence (18.2 J/cm²) and low overlap (85%), the lines exhibited deviations from straightness, primarily due to melting on the ridges. Notably, even for the most intense energy condition (fluence 18.2 J/cm² and overlap 98%), the grooves began losing their definition again. This suggests that ablation and melting were likely taking place. Additionally, the presence of particles, possibly in the form of metal oxides, could be observed within the groove. This was substantiated by the EDS analysis shown in Figure 8. The emergence of larger particles was particularly notable under laser conditions involving low energy (0.9 J/cm²) and high overlap (96% and 98%). The impact of these particles on material properties, as well as the mechanism behind their formation, should be a subject of further investigation in subsequent studies.

Distinct from the CoCrMo alloy, no evidence of LIPSS was discernible in the AZ91D alloy. This disparity can likely be attributed to the pronounced melting that has the potential to disrupt the submicrometric structures.

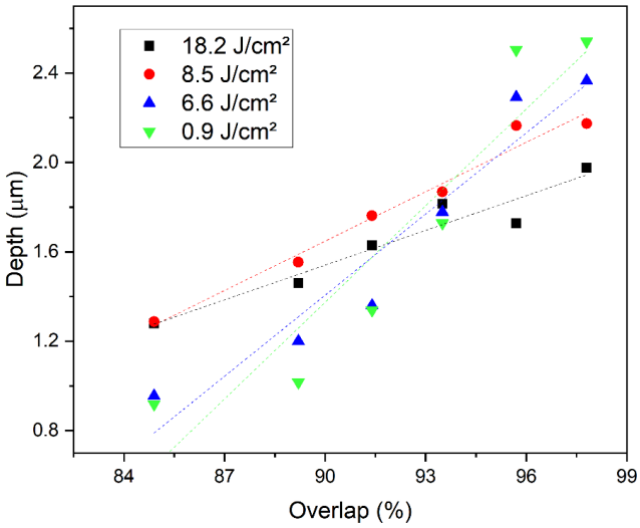

Figure 3. Average depth and standard deviation of the periodic structures as function of the pulse-to-pulse overlap for different values of laser fluences. Reprinted from (Henriques et al., 2023b), Copyright (2023), with permission from MDPI.

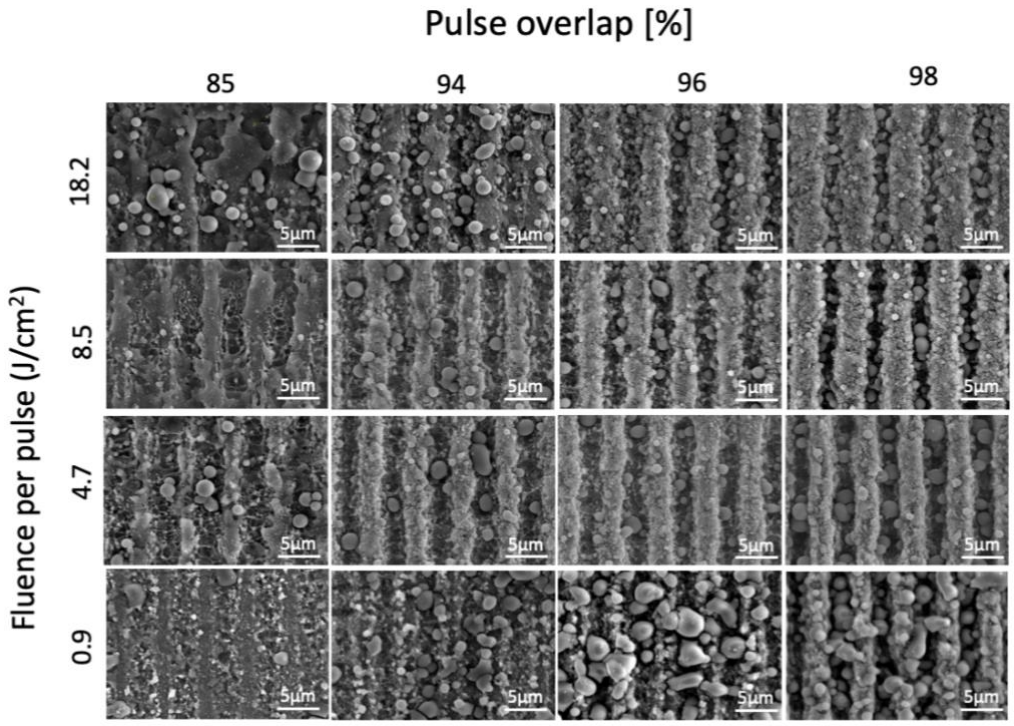

Figure 4. SEM images of the sample's surfaces for each fluence and pulse overlap tested. Reprinted from (Henriques et al., 2023b), Copyright (2023), with permission from MDPI.

3.3. Zirconia (3Y-TZP)

Figure 5 displays the pattern depth variation concerning pulse overlap for various laser fluences. It is evident that as pulse overlap levels increase, and correspondingly, as laser fluences elevate, the pattern depth also experiences a proportional increase. For instance, consider a fluence of 5.7 J/cm²: the depth of the structure steadily rises from 0.3 µm to 1.2 µm when pulse overlaps of 92% and 98% are implemented, respectively.

This upward trend persists for higher laser fluences (such as 7.6 J/cm² and 9.5 J/cm²), even though irregularities within the structures begin to manifest at higher pulse overlaps. These anomalies, arising from ablation at the ridges, are indicated on the graph by an asterisk (*), signifying the specific laser conditions associated with such occurrences.

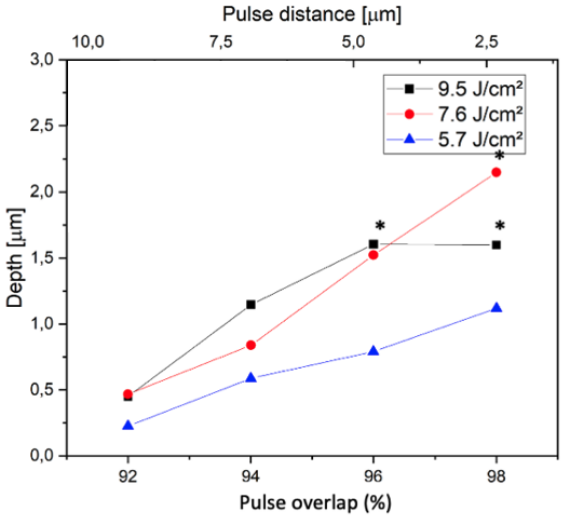

Figure 5. illustrates SEM micrographs of zirconia surfaces treated with lasers under varying combinations of DLIP parameters: pulse fluence ranging from 5.7 to 9.5 J/cm² and pulse-to-pulse (PTP) overlap spanning from 92 to 98%.

At lower energy densities (e.g., 5.7 J/cm²), the resulting patterns exhibit heightened clarity as the pulse overlap levels increase. This progression is evident from a pattern characterized by low structure depths and indistinct shapes at 92% overlap, evolving into a distinctly defined, uniform striped pattern featuring deep valleys and consistent ridges at 98% overlap. In the latter case, well-defined ablated areas stand in stark contrast to the non-ablated regions, featuring sharp boundaries.

This trend persists even at higher energy densities, although a disruption of the structures' ridges becomes noticeable at elevated pulse overlaps (e.g., 98% overlap at 7.6 J/cm²; 98% and 96% overlap at 9.5 J/cm²). Notably, the dominance of the pulse overlap condition in shaping pattern formation becomes evident. This is exemplified by the shallow patterns generated at 92% overlap, irrespective of the employed laser fluence levels.

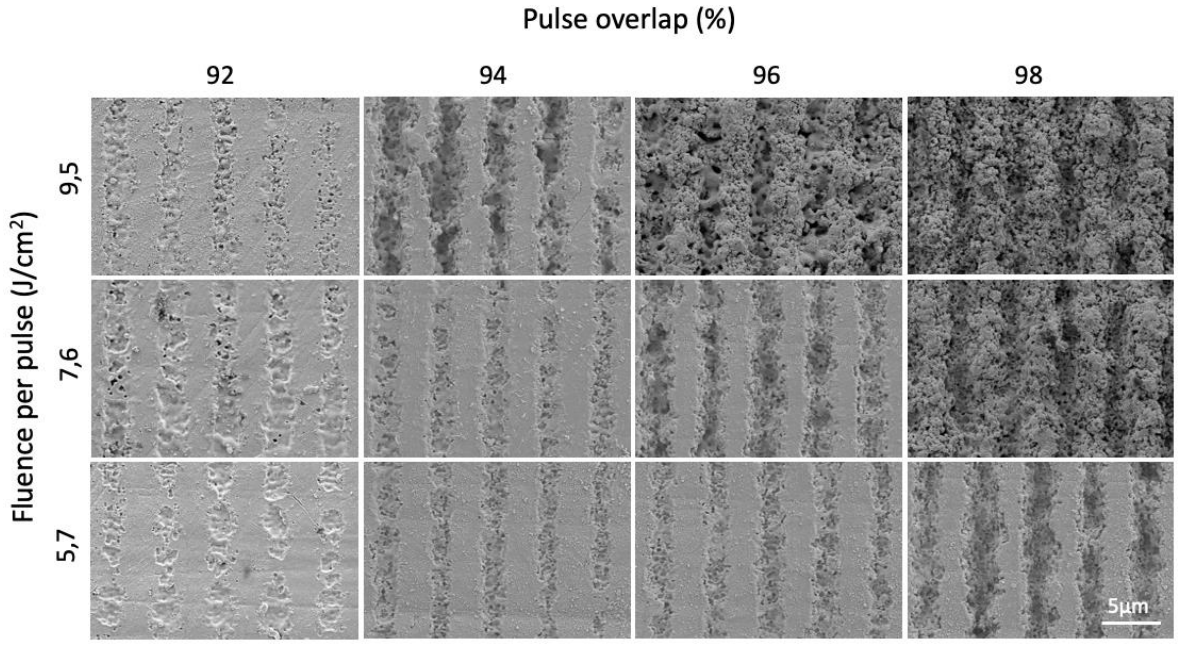

Figure 6. Scanning electron micrographs of the DLIP treated zirconia surfaces with different set of laser parameters: laser fluence and pulse overlap. Laser fluence increases from bottom to top and pulse overlap increases from left to right.

3.4. Poly-ether-ether-ketone (PEEK)

In Figure 7, the relationship between pattern depth and pulse overlap is graphically represented for different laser fluences. It is evident that an escalation in pattern depth correlates with higher pulse overlap levels, as well as increased laser fluence values. To elucidate, consider a fluence of 8.5 J/cm²: under this circumstance, the depth of the structure exhibits a gradual ascent from 1.6 µm to 2.4 µm, as the pulse overlap shifts from 83% to 91%. Similarly, when maintaining the pulse overlap at 89%, the structure depth similarly demonstrates an upward trend in relation to higher laser fluence values. For instance, starting at 1.7 µm at 6.6 J/cm², it progresses to 2.2 µm at 8.5 J/cm², culminating at 2.6 µm for 11.4 J/cm².

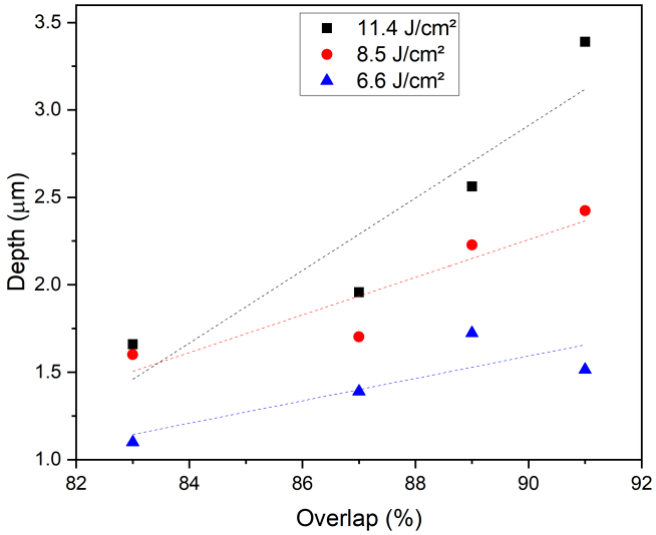

Figure 7. Mean pattern depth of the DLIP structures produced in PEEK surface for a different set of laser parameters: laser fluence in the range of 6.6 to 11.4 J/cm² and pulse overlap in the from 83 to 91 %. Reprinted from (Henriques et al., 2023a), Copyright (2023), with permission from Elsevier.

In Figure 8, SEM micrographs show DLIP-treated PEEK surfaces, each exhibiting distinct combinations of laser parameters: pulse fluence spanning from 6.6 to 11.4 J/cm² and pulse overlap (Ov) ranging from 83% to 91%. Observing the images, it becomes evident that at lower Ov values (83%), the initial stages of structure formation commence, albeit with indistinct groove definition, regardless of the fluence level. Conversely, higher Ov levels yield more uniform structures characterized by deeper grooves, irrespective of the fluence employed. For instance, structures manifest at fluence levels of 6.6 J/cm², 8.4 J/cm², and 11.4 J/cm², accompanied by Ov values of 87%, 89%, and 87%, respectively. Moreover, it was discovered that excessive destruction of structures transpired at notably elevated levels of Ov and fluence (e.g., 11.4 J/cm² and 91% Ov).

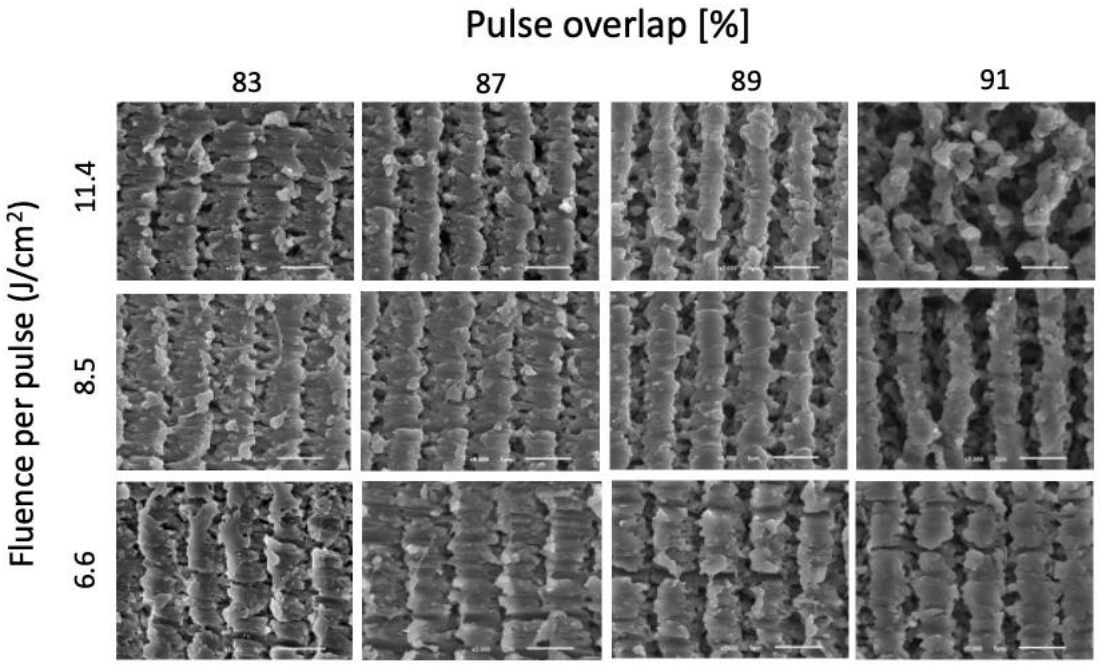

Figure 8. Scanning electron micrographs of the DLIP-treated PEEK surfaces with a different set of laser parameters: laser fluence and pulse overlap. Laser fluence increases from bottom to top, and pulse overlap increases from left to right. Reprinted from (Henriques et al., 2023a), Copyright (2023), with permission from Elsevier.

4. CONCLUSIONS

This study explored the creation of DLIP structures utilizing an ultra-short pulse infrared laser source (wavelength: 1064 nm, pulse duration: 10 ps) on AZ91D magnesium, CoCrMo alloy, PEEK and Zirconia (3Y-TZP). The research also delved into assessing how laser parameters impact the structural morphology. The following conclusions can be drawn from this study:

- Line-like designs characterized by a periodic repetition of $\lambda = 5.0$ µm were successfully generated by employing a full beam angle of 24º in all the materials tested.
- DLIP proved capable of generating uniform line-like structures characterized by a spatial period of 5 µm and depths reaching up to 0.85 µm for the CoCrMo alloy. Additionally, under high-energy conditions, the presence of sub-micrometric secondary structures, which can be identified as LIPSS, was observed.
- In the context of the AZ91D alloy, the successful fabrication of line-like structures with a periodicity of 5 µm and an average depth ranging from 0.9 µm to 2.5 µm—deeper than those achieved on the CoCrMo alloy—was achieved.
- In zirconia surfaces, pattern depths, reaching heights of up to 1.5 µm, were attained using specific parameters, such as 7.6 J/cm² and 96% overlap.
- Mean depths reaching approximately ~2.5 µm (yielding an aspect ratio of ~0.5) were achieved in PEEK substrates. Notably, these structures encompassed secondary formations, namely laser-induced periodic surface structures (LIPSS), characterized by a spatial periodicity of approximately ~1 µm.

5. ACKNOWLEDGMENTS

This study was supported by the Capes-Humboldt Research Fellowship Programme (Ref: 88881.197684/2018-01), FCT-Portugal (through the reference projects UIDB/04436/2020 and UIDP/04436/2020)), by the Capes/DAAD PROBRAL Programme (Ref: 88887.628082/2021-00), FINEP-Brazil (Project BIOMIO – 01.22.0180.00 (0027/21)), and Foundation for the Support of Research and Innovation of the State of Santa Catarina – FAPESC (ref. 2021TR001461).

6. REFERENCES

Aguilar-Morales, A.I., Alamri, S., Lasagni, A.F., 2018. Micro-fabrication of high aspect ratio periodic structures on stainless steel by picosecond direct laser interference patterning. J. Mater. Process. Technol. 252, 313–321. https://doi.org/10.1016/j.jmatprotec.2017.09.039

Bauer, F., Michalowski, A., Kiedrowski, T., Nolte, S., 2015. Heat accumulation in ultra-short pulsed scanning laser ablation of metals. Opt. Express 23, 1035. https://doi.org/10.1364/OE.23.001035

Bohinc, K., Dražić, G., Fink, R., Oder, M., Jevšnik, M., Nipič, D., Godič-Torkar, K., Raspor, P., 2014. Available surface dictates microbial adhesion capacity. Int. J. Adhes. Adhes. 50, 265–272. https://doi.org/10.1016/j.ijadhadh.2014.01.027

Brown, M.S., Arnold, C.B., 2010. Fundamentals of Laser-Material Interaction and Application to Multiscale Surface Modification, in: Springer Series in Materials Science. Springer, Berlin, Heidelberg, pp. 91–120. https://doi.org/10.1007/978-3-642-10523-4_4

Cunha, A., Elie, A.-M., Plawinski, L., Serro, A.P., Botelho do Rego, A.M., Almeida, A., Urdaci, M.C., Durrieu, M.-C., Vilar, R., 2016. Femtosecond laser surface texturing of titanium as a method to reduce the adhesion of Staphylococcus aureus and biofilm formation. Appl. Surf. Sci. 360, 485–493. https://doi.org/10.1016/j.apsusc.2015.10.102

Dumas, V., Rattner, A., Vico, L., Audouard, E., Dumas, J.C., Naisson, P., Bertrand, P., 2012. Multiscale grooved titanium processed with femtosecond laser influences mesenchymal stem cell morphology, adhesion, and matrix organization. J. Biomed. Mater. Res. - Part A 100, 3108–3016. https://doi.org/10.1002/jbm.a.34239

El-Khoury, M., Alamri, S., Voisiat, B., Kunze, T., Lasagni, A.F., 2020. Fabrication of hierarchical surface textures using multi-pulse direct laser interference patterning with nanosecond pulses. Mater. Lett. 258, 126743. https://doi.org/10.1016/j.matlet.2019.126743

Henriques, B., Fabris, D., Voisiat, B., Lasagni, A.F., 2023a. Multi-scale textured PEEK surfaces obtained by direct laser interference patterning using IR ultra-short pulses. Mater. Lett. 339, 134091. https://doi.org/10.1016/j.matlet.2023.134091

Henriques, B., Fabris, D., Voisiat, B., Lasagni, A.F., 2023b. Multi-Scale Structuring of CoCrMo and AZ91D Magnesium Alloys Using Direct Laser Interference Patterning. Metals (Basel). 13, 1248. https://doi.org/10.3390/met13071248

Le Guéhennec, L., Soueidan, A., Layrolle, P., Amouriq, Y., 2007. Surface treatments of titanium dental implants for rapid osseointegration. Dent. Mater. https://doi.org/10.1016/j.dental.2006.06.025

Lukaszewska-Kuska, M., Wirstlein, P., Majchrowski, R., Dorocka-Bobkowska, B., 2018. Osteoblastic cell behaviour on modified titanium surfaces. Micron 105, 55–63. https://doi.org/10.1016/j.micron.2017.11.010

Mücklich, F., Lasagni, A., Daniel, C., 2006. Laser interference metallurgy - Using interference as a tool for micro/nano structuring. Int. J. Mater. Res. 97, 1337–1344. https://doi.org/10.3139/146.101375

Mulko, L., Soldera, M., Lasagni, A.F., 2022. Structuring and functionalization of non-metallic materials using direct laser interference patterning: a review. Nanophotonics 11, 203–240. https://doi.org/10.1515/nanoph-2021-0591

Schieber, R., Lasserre, F., Hans, M., Fernández-Yagüe, M., Díaz-Ricart, M., Escolar, G., Ginebra, M.-P., Mücklich, F., Pegueroles, M., 2017. Direct Laser Interference Patterning of CoCr Alloy Surfaces to Control Endothelial Cell and Platelet Response for Cardiovascular Applications. Adv. Healthc. Mater. 6, 1700327. https://doi.org/10.1002/adhm.201700327

Stark, T., Alamri, S., Aguilar-Morales, A.I., Kiedrowski, T., Lasagni, A.F., 2019. Positive Effect of Laser Structured Surfaces on Tribological Performance. J. Laser Micro/Nanoengineering. https://doi.org/10.2961/jlmn.2019.01.0003

Watanabe, H., Saito, K., Kokubun, K., Sasaki, H., Yoshinari, M., 2012. Change in surface properties of zirconia and initial attachment of osteoblastlike cells with hydrophilic treatment. Dent. Mater. J. 31, 806–814. https://doi.org/10.4012/DMJ.2012-069